High-Energy-Density Foldable Battery Enabled by Zigzag-Like Design

Xiangbiao Liao, Changmin Shi, Tianyang Wang, Boyu Qie, Youlong Chen, Pengfei Yang, Qian Cheng, Haowei Zhai, Meijie Chen, Xue Wang, Xi Chen,* and Yuan Yang*

Flexible batteries, seamlessly compatible with flexible and wearable electronics, attract a great deal of research attention. Current designs of flexible batteries struggle to meet one of the most extreme yet common deformation scenarios in practice, folding, while retaining high energy density. Inspired by origami folding, a novel strategy to fabricate zigzag-like lithium ion batteries with superior foldability is proposed. The battery structure could approach zero-gap between two adjacent energy storage segments, achieving an energy density that is 96.4% of that in a conventional stacking cell. A foldable battery thus fabricated demonstrates an energy density of 275 Wh L^{-1} and is resilient to fatigue over 45 000 dynamic cycles with a folding angle of 130°, while retaining stable electrochemical performance. Additionally, the power stability and resilience to nail shorting of the foldable battery are also examined.

1. Introduction

Wearable electronics have attracted increasing attention in the applications of health care[1–3] and sensing devices.[4] Despite the upcoming success of commercialization of flexible displays and epidermal electronics,[3] the lack of deformable power sources represents a serious bottleneck for the deployment of wearable electronics. Since the energy-storage systems (i.e., batteries) must be conformal to complex deformations of flexible electronics, their capabilities of flexibility have been a focal point of research. In recent years, considerable efforts have been made to improve the deformability of lithium ion batteries (LIBs),[1,5,6] the current mainstream of power source. Various efforts have

been devoted to enhance the flexibility of electrodes of LIBs, such as making them slim,[7] incorporate carbon-based[8] and polymer-based conductive materials, etc.[9] Additionally, new electrode architectures such as sponge,[10] textile,[11] and wire-like shapes[12] have been fabricated, showing both improved electrochemical performance and mechanical robustness.

Besides the advance of battery components, new schemes of system-level integration of LIBs with deformability were proposed, which are perhaps more compatible with standard manufacturing process and cost effective. By decoupling the energy storage and deformable parts, highly deformable LIBs have been fabricated.[5,13,14] Stretchable and bendable LIBs were assembled through a segment design of electrode disks connected by a self-similar soft serpentine structure,[15] aided by origami-patterned electrodes.[16] Nevertheless, due to the excessive use of the deformable segment, the mass loading of active materials was low and the cost for assembly was high. Although our previous spine-like design achieved simultaneously both flexibility and high energy density with 86.1% of a standard pouch cell, the system was unable to accommodate escalating deformation, such as folding, while maintaining high energy density, since the design must sacrifice active materials and give room to more deformable parts in order to undergo larger deformation.[13] During fabrication, the complex cutting of comb-like pattern not only causes incomplete

X. B. Liao, Prof. X. Chen
Yonghong Zhang Family Center for Advanced Materials
for Energy and Environment
Department of Earth and Environmental Engineering
Columbia University
New York, NY 10025, USA
E-mail: xichen@columbia.edu
C. M. Shi, T. Y. Wang, B. Y. Qie, Dr. Q. Cheng, H. W. Zhai,
M. J. Chen, X. Wang, Prof. Y. Yang
Program of Materials Science and Engineering
Department of Applied Physics and Applied Mathematics
Columbia University
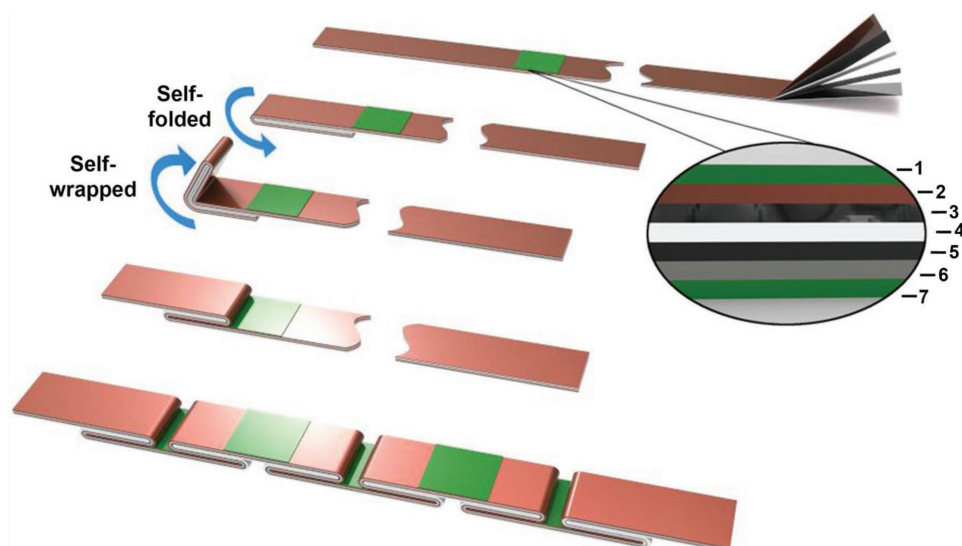New York, NY 10025, USA
E-mail: yy2664@columbia.edu

Y. L. Chen, P. Yang
School of Aerospace
Xi'an Jiaotong University
Xi'an 710049, P. R. China
M. J. Chen
School of Energy Science and Engineering
Harbin Institute of Technology
Harbin 150001, P. R. China
X. Wang
School of Astronautics
Harbin Institute of Technology
Harbin 150001, P. R. China

**ADVANCED
SCIENCE NEWS**
www.advancedsciencenews.com

**ADVANCED
ENERGY
MATERIALS**
www.advenergymat.de

**1/7: Tape; 2: Copper Substrate; 3: Graphite (Anode); 4: Seperator;
5: Lithium cobalt oxide (Cathode); 6: Aluminum Substrate.**

Figure 1. Fabrication process of the zigzag-like foldable battery.

utilization of electrode sheets, but also increases the cost. A drastically new system design is urgently needed, which may simultaneously incorporate high energy density and tolerance to extreme deformation (such as foldability), hence calling the need for more efficient coupling between energy storage and deformable parts, as well as simplifying the fabrication process and being more cost effective for scale-up industrial production of flexible LIBs.

Herein, inspired by origami folding, we design a facile approach to fabricate novel flexible LIBs with superior foldability and high energy density. As shown in **Figure 1**, the conventional graphite anode/separator/ lithium cobalt oxide (LCO) cathode stack maintains its integrity and being simply folded into strip-like origami segments, connected by division segments (3 mm in length, green in Figure 1) which serve as future folding joints. To protect these "weak points" that may undergo excessive deformation and fatigue in practice, protective thin tape is adopted to cover metal foils in these division joints (and on both sides). The tape is only applied to joint area, which only occupies less than 4% of the area, so it sacrifices little energy density (e.g., < 0.5%). Note that within a stack, the spacing between division joints may be varied, which affects energy density and foldability and is discussed later. The main energy storage is borne by the alternatively self-folded and self-wrapped origami strips, which are much thicker and rigid compared to the division joints. Such an assembly strategy not only allows superior foldability (thanks to the flexible and tough division joints) and attains high energy density (since the gap between two thick segments may approach zero when folded), but also the fabrication process is simple and easy to scale up, since the integrity of the entire stack is well maintained.

The cell thus fabricated with energy density of 275 Wh L^{-1} can reach 96.4% of the conventional stacking cell using the same parameters. The zigzag-like structural design could accommodate up to 180° folding between the two rigid origami units, although a small gap between the thick stacking segments is needed in practice (to accommodate packaging and provide extra tolerance to large deformation, and such a gap is typically ≈1.0 mm). The cell also performs well under cyclic charging and fatigue cycles: after over 100 cycles of charge/discharge at 0.5 C, 96% battery capacity remained even under alternative bending deformations. After 45 000 cycles of continuously dynamic folding loads, the discharge capacity of 124.2 mAh g^{-1} is survived at 1 C (1 C = 145 mAh g^{-1}). Furthermore, no smoke or fire is observed when the cell is shorted by a stainless steel nail. Therefore, this novel zigzag-like battery structure and its facile fabrication may attract great promise for practical applications in flexible battery with superior foldability.

2. Structure–Mechanical Property Relation

Optimization of structural design in such zigzag-like battery is required to realize excellent flexibility while maintaining electrochemical performances in practice. With the present asymmetric zigzag-like structure, the best folding deformation should follow that in Scheme A in **Figure 2**a, where the two adjacent joints are bent in opposite directions. The unidirectional bending (Scheme B) is also acceptable although the overall folding angle is limited at one joint. Scheme C, however, should be avoided in practice since it may cause deleterious stretch in the joints and contact stress between two thick stacking segments.

To show the mechanical foldability and durability of the cell, finite element calculations are carried out to evaluate the deformation at folding joints. The result in Figure 2b shows that the zigzag-like structure with zero gap can be folded by 180° (by following Scheme A) and become self-compacted, and the smallest bending diameter d_0 at folding joints is 0.3 L.
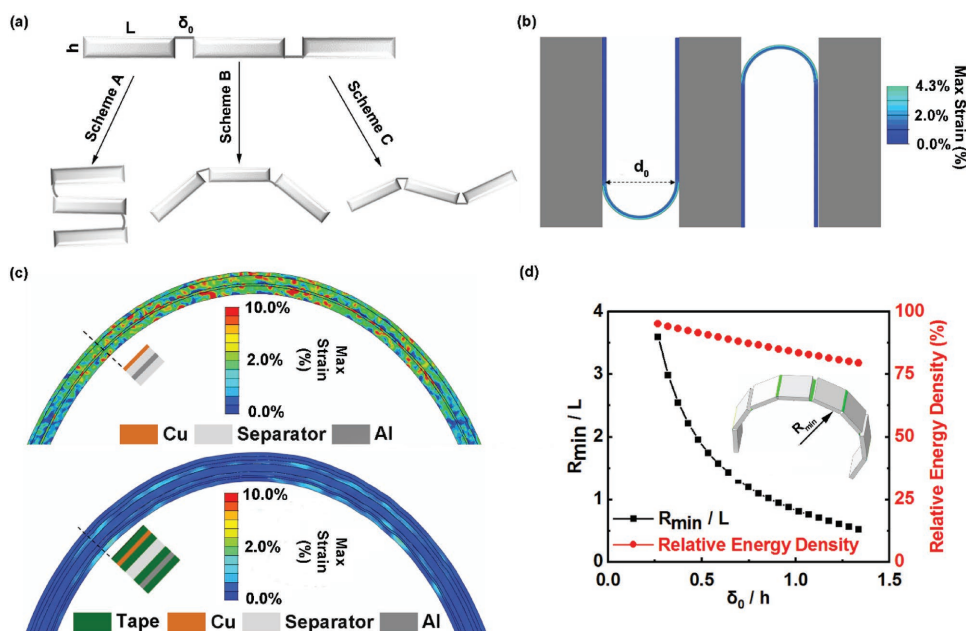
Figure 2. Structural design for the zigzag foldable battery. a) Geometrical schematic and three main operational schemes of the battery. b) Folding deformation of zigzag-like battery structure with a bending diameter of 3 mm where the tape length is half of stack length. c) Strain contours of electrode multilayers at folding joints without (top) and with (bottom) protective tapes. d) Relative minimum bending radius and relative energy density as a function of dimensionless gap width δ_0/h for unidirectional bending.

Here, L is the length of the thick stack (1 cm for the fabricated battery), and h is its thickness. Figure 2c shows the strain contours of multilayer stack at joints with and without protective tapes under 180° folding deformation. Since large shear deformation is borne by the soft components (tapes and separators), the maximum strain in metal foil (e.g., aluminum) is only 0.5% with the presence of protective tape, much smaller than that (5.5%) for the naked joint. Therefore, the adhesive tape covering both sides of the folding joints is capable for enhancing the mechanical durability of flexible battery upon continuous folding.

In case some battery joints are bent in an undesired direction, e.g., unidirectional bending in Scheme B, a necessary gap length (δ_0) of the joint is needed to tolerate excessive deformation and contact between stacking units (whose thickness is h), but unavoidable of sacrificing its energy density. The balance between acceptable bending radius (beyond which excessive stretch can damage joints) and relative energy density is sought after in Figure 2c. When $\delta_0/h = 0.5$, the minimum dimensionless bending radius for Scheme B is $R_{min}/L = 1.7$ with uniform bending imposed at each joint, and a high relative energy density of 91% can be retained, compared with the battery without the foldable part but having the same parameters. However, for the operation in Scheme C, owing to excessive segment contact or joint stretching, the acceptable folding angles at joints are only 34° and 15° for exemplified parameters $\delta_0/h = 0.5$ and $\delta_0/h = 0.25$, respectively. Therefore, the requirements for function-oriented operations of such zigzag-like battery are highly dependent on the geometric design and deployment strategy. Systematic designs, including tape thickness, property, origami pattern, etc., are subjected to future study.

3. Electrochemical Performance of Foldable Batteries

In order to demonstrate the electrometrical performance of the foldable battery, a full cell (LiCoO$_2$ (LCO)/Graphite) was tested at 0.5 C, while under various mechanical deformation configurations (Figure S1, Supporting Information) for 100 cycles. As shown in **Figure 3**a, the battery was first run in the flat configuration (region I, Figure S1a, Supporting Information) for 15 cycles. Its capacity slightly decayed from 148.6 to 147.2 mAh g^{-1} (0.06% per cycle). Then, the battery was manually bent as Scheme B with a diameter of ≈2 cm ($D = 2$ cm, Figure S1b, Supporting Information) for 1000 times, and then it was cycled in the bent configuration ($D = 6$ cm, Figure S1c, Supporting Information) in region II. The discharge capacity first increased to 148.5 mAh g^{-1} after flexing, and remained at 146.5 mAh g^{-1} after 10 cycles. After a flat relaxation in region III, the battery was then tested in the flexed configuration (region IV, Figure S1d, Supporting Information), associated with bending 1000 times (Scheme B, $R_{min}/L = 1$) in advance. The capacity loss in region IV was only 0.06% per cycle, which was the same as that in the flat state (region I). This implied that the repetitive mechanical deformations have almost no impact on the as-designed foldable battery. After being folded (90°) 1000 times following Scheme A (Figure S1e, Supporting Information), the battery was subjected to folded (90°) configuration (region VI), and the total capacity loss was only 1.7 mAh g^{-1}, corresponding to 0.077% loss per cycle. Subsequently, the cell undergone 180° manual folding for 1000 times (Scheme A), followed by cycling at the static 180° folded configuration for 20 cycles (region VIII, Figure S1f, Supporting Information). The total capacity loss was small (1.4 mAh g^{-1}). It is clear that the electrochemical

**ADVANCED
SCIENCE NEWS**

www.advancedsciencenews.com

**ADVANCED
ENERGY
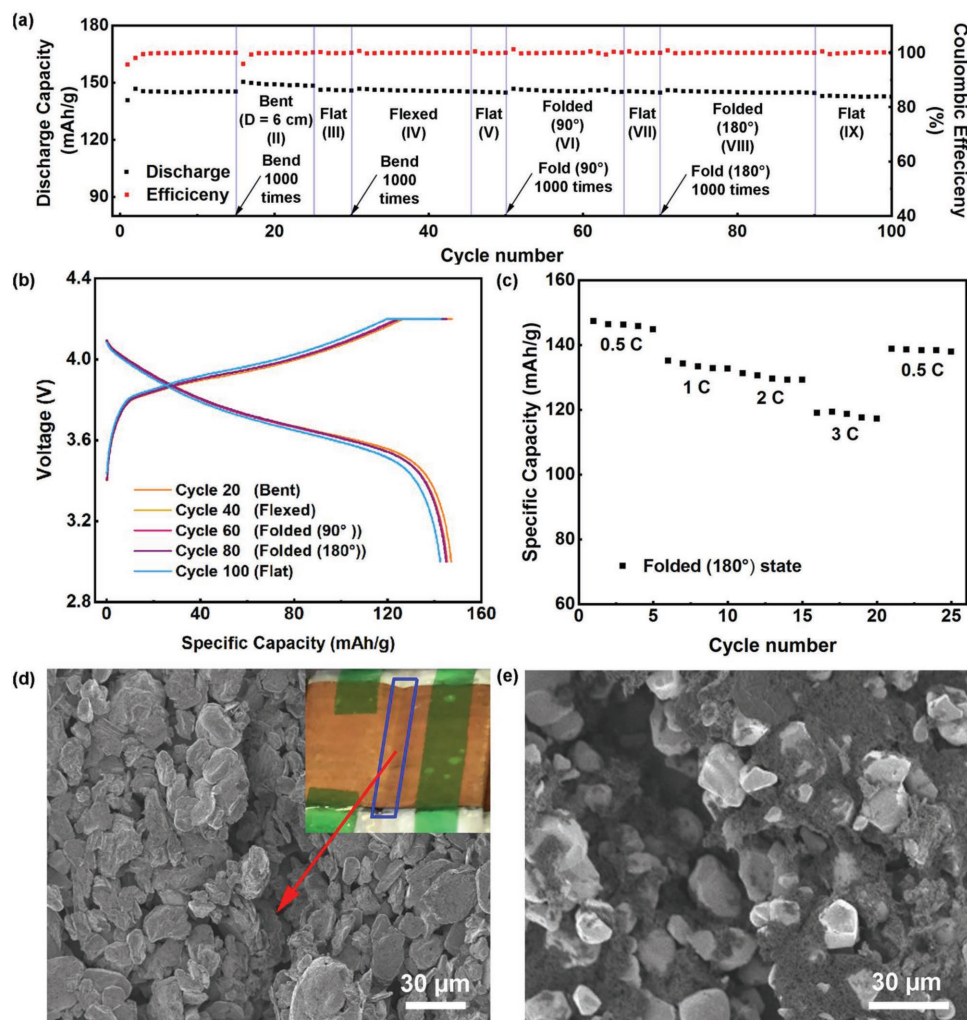MATERIALS**

www.advenergymat.de

Figure 3. The electrochemical performance of the foldable battery undergoing different types of deformations. a) Cycling performance in various deforming configurations during 0.5 C charge/discharge for 100 cycles. b) Galvanostatic charge–discharge profiles at different configurations: the 20th, 40th, 60th, 80th, and 100th cycles. c) Rate performance of the foldable battery at high current density ranging from 0.5 to 3 C and then back to 0.5 C at folded (180°) configuration. d,e) Scanning electron microscopy (SEM) images of (d) graphite and (e) LCO layers at the folding joint.

performance was almost unchanged under such harsh folding. Finally, the battery was released into flat configuration (region IX) and steadily ran the last five cycles. Even after having undergone alternative harsh deformations, a high capacity retention of 96% with an average Coulombic efficiency better than 99.9% after 100 cycles was achieved. The outstanding cycling performance indicates that such a foldable battery with novel zigzag structure is highly resistant to deformations, as the zigzag structure decouples thick energy storage component and thin folding joints, so that most part of electrodes are not subjected to mechanical stress. In addition, an interesting phenomenon observed is that the capacity always increases slightly after bending. This can be attributed to better electrolyte wetting caused by mechanical deformation and better contact among electrode particles and current collectors in the bent state.

To intuitively present the capacity change, Figure 3b shows the voltage profiles in different cycles, demonstrating little fading in the specific capacity and overpotential. In addition, electrochemical impedance spectroscopy (EIS) was applied

to further understand the robustness of the foldable battery. The charge transfer resistance changed slightly from 3.27 to 3.36 Ω (Figure S2, Supporting Information), which implies that the foldable battery is robust enough to bear mechanical deformations.

Practical applications on wearable electronic devices necessitate stable output power under large charging/discharging current. To evaluate the electrochemical performance at high current density, a full cell was fixed into a harshly folded (180°) configuration and continuously cycled at 0.5, 1, 2, 3 C and then back to 0.5 C with five cycles for each C-rate (Figure 3c). It is demonstrated that the capacity decreased steadily, corresponding to a reduction of 17% totally from 0.5 to 3 C. Finally, the current density was switched back to 0.5 C after the galvanostatic charge/discharge at 3 C. The total capacity changed from 147.3 to 137.9 mAh g^{-1} (capacity retention was 93.6%) after 25 such cycles. The electrochemical stability and recoverability are insensitive to high current density, which illustrates that the proposed foldable battery is attractive in powering

commercial applications. In fact, the capacity stability at high C-rate is due to the zigzag-like design that enables tight contact between different layers, which can prevent electrode materials from peeling off from their substrates. Furthermore, the above deformed and cycled cell was disassembled to examine the morphology of both graphite and LCO layers at folding joints (Figure S3, Supporting Information) where they underwent largest deformation. Although crease with width <50 µm is observed, no delamination is detected at both cathode and anode. The crease also does not propagate after another 2000 folding cycles (Figure S4, Supporting Information) as 50 µm is much smaller than the distance between two folding joints (≈7 cm). This indicates very little impact on cell performance, which is also supported by the steady cycling data in Figure 3a. More discussion can be found in the Supporting Information.

To further illustrate its applications in wearable devices, the durability of the foldable battery under repetitive folding for over thousands of cycles is crucial. Here, we tested the electrochemical performance of our battery while simultaneously conducting a dynamic loading experiment, where one end of the battery was fixed and the other end was bent back and forth by one actuator, which folded the battery repetitively by 130°. As shown in **Figure 4**a, the full cell was charged/discharged flatly for the first five cycles at 1 C, and it was then cycled under the dynamic loading for the next 15 cycles. During the experiment, the frequency of transition between the flat and folded (130°) state was 0.5 Hz, which represents 45 000 folding–unfolding times during 15 charging/discharging cycles at 1 C. The voltage change on discharge was less than 5 mV (Video S1, Supporting

Information). During these 15 cycles, the capacity subtly changed from 139 to 124.2 mAh g^{-1} with 0.7% loss per cycle, and the average Coulombic efficiency was above 99.6%. Specifically, the capacity was reduced by 0.38% from the cycle 16 to cycle 20. Illustrated by the voltage profiles in Figure 4b, no apparent change in voltage profile was observed. For comparison, a conventional stacking cell that had the same parameters was fabricated, and its electrochemical performance was also tested. Under a dynamic and small folding angle (30°) deformation with even lower frequency (0.05 Hz), the discharging voltage fluctuated significantly ranging from 4.2 to 3.4 V. Comparing to the conventional stacking cell, our flexible battery design only suffered little strain in its electrodes during folding and the active materials and metal foil remained stable contact, enabling its high electromechanical stability.

4. Application Demonstration

To demonstrate its practical application, a fully charged zigzag-like foldable battery was used to power a series of light emitting diode (LEDs) lights. First, the cell was fully charged at 0.5 C with theoretical energy density up to 275 Wh L^{-1}, and then continuously folded by 90° and 180° (Scheme A) during discharge period. After one folding, the cell was flattened back. **Figure 5**a shows that the voltage fluctuation during the discharge period is less than 1 mV, which implies small resistance change of less than 0.5% (0.04 Ω/8 Ω). Subsequently, the LEDs showing a "CU" pattern were
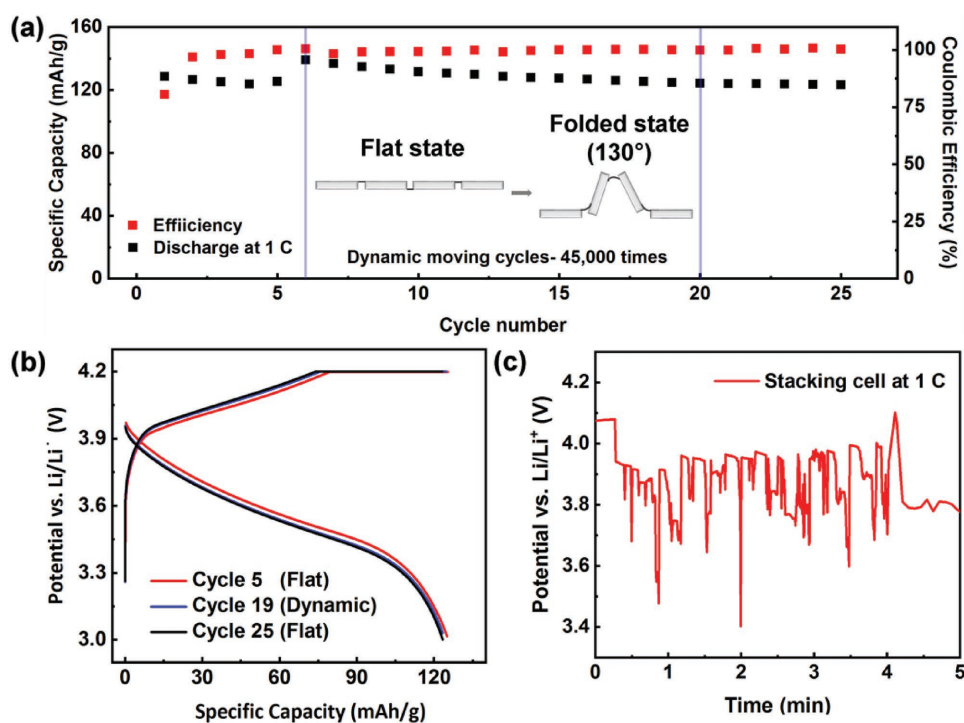

Figure 4. Dynamic loading test of the foldable battery at 1 C. a) Cycling performance of a zigzag-like foldable battery in different states under dynamic and repetitive fold loading test. The inset shows the schematic of the flat and folding configurations. b) Galvanostatic charge–discharge voltage profiles for 5th, 19th, and 25th cycle. c) The discharge profile of a normal stacking cell at 1 C, subjected to lower folding frequency.
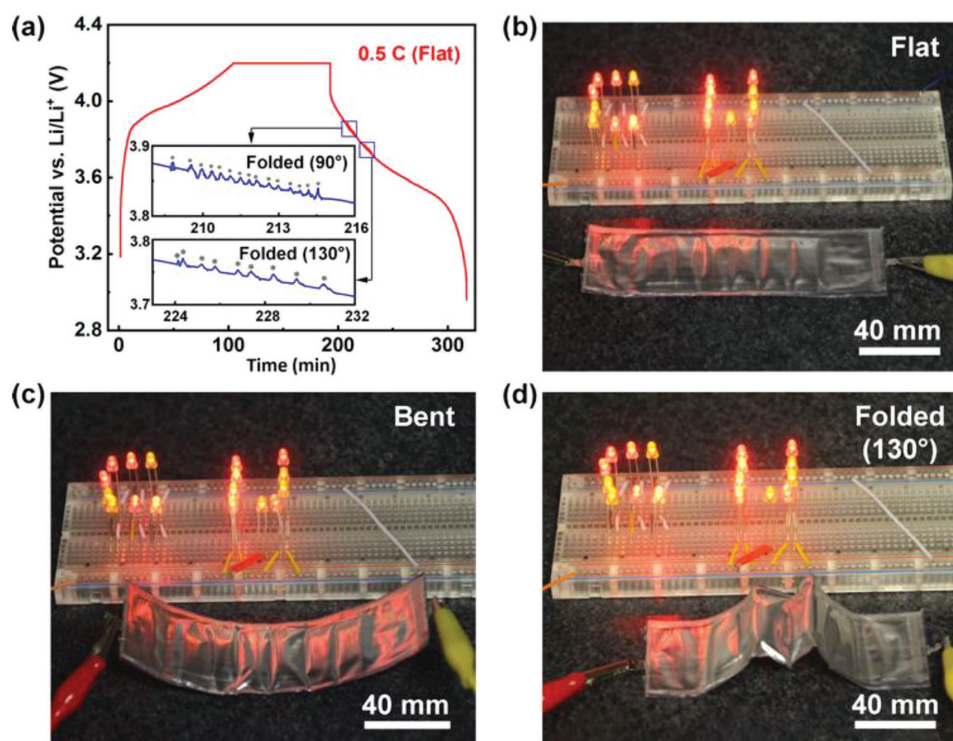
Figure 5. a) Voltage profile for the foldable battery under continuously and manually 90° and 180° folding during discharge. b–d) Practical applications of foldable battery to power a series of LEDs in flat, bent, and folded configurations.

powered by the foldable battery in flat, bent, and folded (130°) configurations, shown in Figure 5b, 5c, and 5d, respectively. Regardless of deformations in the battery, the brightness of these LEDs remained unchanged. Furthermore, the same functionality was maintained when continuously harsh folding was applied (Video S2, Supporting Information), which implies that our design is applicable to commercial use. Apart from stable electromechanical performance, safety is crucial to be addressed for applications. In our experiment, the foldable battery was fully charged at 0.5 C and then it was punctuated by a nail (Figure S5a,b, Supporting Information). The voltage dropped to zero once nail penetration without any smoke or fire observed (Video S3, Supporting Information). The thermal stability is possibly due to our zigzag-like battery design, which stores energy in distributed units.

5. Conclusion

In conclusion, we proposed a facile strategy to fabricate zigzag-like LIB with superior foldability, high energy density, and excellent electrochemical performance and mechanical endurance. The zigzag-like battery can be well fitted to many operation scenarios. The as-constructed battery has an energy density of 275 Wh L^{-1}, which is 96.4% compared with a conventional cell. In addition, even after different mechanical deformations at 0.5 C for 100 cycles, the foldable battery can still remain 96% with an average Coulombic efficiency higher than 99.9%. More importantly, this cell could withstand extreme dynamic folding operation (130° for 45 000 times) while maintaining stable

capacity at 1 C, demonstrating promising potential practical applications.

6. Experimental Section

Mechanical Simulation: The deformation of zigzag-like battery using 2D nonlinear finite element method, implemented in the commercial software ABAQUS, was simulated.[17] In all cases, four-node quadrilateral stress/displacement elements with reduced integration were used. The energy storage units were considered as rigid parts and the sheet of folding joints was the stack of tape/anode/tape/double separators/tape/aluminum foil/tape. For simplicity, linear isotropic elasticity was adopted for the battery structure with effective modulus and Poisson ratio based on experimental parameters. The length and thickness of joint layers were 6 mm and 132 µm, respectively. For each layer in terms of thickness, tape was 32 µm. Cu foil: 18 µm; Al foil: 24 µm, and separator was 25 µm. The pressure of 1 atm was applied to both sides of deformable layers to simulate the vacuum conditions inside the aluminized pouch bag. The originally flat origami-inspired structure was subjected to angle displacement load for realizing folding configuration.

Battery Fabrication: Commercial LiCoO$_2$ and graphite electrodes (Custom Electronics Inc.) were used as cathode and anode, respectively. Then the electrodes and separators (Celgard 2500) were cut into required size. Protective tap was used to enhance the ability of large folding. After that, the aluminized polyethylene (Sigma–Aldrich) package was used to pack the battery and then transferred into the argon-filled glove box (O$_2$ < 0.1 ppm, H$_2$O < 0.1 ppm) to drop ethylene carbonate/diethyl carbonate (1:1 vol/vol) (Gotion Corp.) electrolyte. After resting for 6 h, the aluminized polyethylene package was vacuum sealed using a high temperature sealer. The total length and width of the cell were 61.1 and 1.5 mm, respectively and each unit was 7 mm long.

Electrochemical Tests: The foldable LCO/Graphite batteries were firstly charged to 4.2 V and held at 4.2 V until the current density decreased

**ADVANCED
SCIENCE NEWS**

www.advancedsciencenews.com

**ADVANCED
ENERGY
MATERIALS**

www.advenergymat.de

to 0.05 C to ensure the batteries could be fully charged. The cut-off voltage of discharge was 3.0 V. The batteries were tested using the battery analyzers of Landt Instruments (Model: CT 2001) and Bio-logic Potentiostat (Model: VMP3).

Conflict of Interest

The authors declare no conflict of interest.

[1] a) A. M. Gaikwad, B. V. Khau, G. Davies, B. Hertzberg, D. A. Steingart, A. C. Arias, *Adv. Energy Mater.* **2015**, *5*, 1401389; b) G. Zhou, F. Li, H.-M. Cheng, *Energy Environ. Sci.* **2014**, *7*, 1307.

[2] D. H. Kim, N. Lu, R. Ghaffari, Y. S. Kim, S. P. Lee, L. Xu, J. Wu, R. H. Kim, J. Song, Z. Liu, J. Viventi, B. de Graff, B. Elolampi, M. Mansour, M. J. Slepian, S. Hwang, J. D. Moss, S. M. Won, Y. Huang, B. Litt, J. A. Rogers, *Nat. Mater.* **2011**, *10*, 316.

[3] D.-H. Kim, N. Lu, R. Ma, Y.-S. Kim, R.-H. Kim, S. Wang, J. Wu, S. M. Won, H. Tao, A. Islam, K. J. Yu, T. I. Kim, R. Chowdhury, M. Ying, L. Xu, M. Li, H. J. Chung, H. Keum, M. McCormick, P. Liu, Y. W. Zhang, F. G. Omenetto, Y. Huang, T. Coleman, J. A. Rogers, *Science* **2011**, *333*, 838.

[4] a) Y. Khan, A. E. Ostfeld, C. M. Lochner, A. Pierre, A. C. Arias, *Adv. Mater.* **2016**, *28*, 4373; b) J. S. Kim, D. Ko, D. J. Yoo, D. S. Jung, C. T. Yavuz, N. I. Kim, I. S. Choi, J. Y. Song, J. W. Choi, *Nano Lett.* **2015**, *15*, 2350; c) L. Peng, X. Peng, B. Liu, C. Wu, Y. Xie, G. Yu, *Nano Lett.* **2013**, *13*, 2151; d) F. Schedin, A. K. Geim, S. V. Morozov, E. W. Hill, P. Blake, M. I. Katsnelson, K. S. Novoselov, *Nat. Mater.* **2007**, *6*, 652.

[5] K. K. Fu, J. Cheng, T. Li, L. Hu, *ACS Energy Lett.* **2016**, *1*, 1065.

[6] H. Gwon, J. Hong, H. Kim, D.-H. Seo, S. Jeon, K. Kang, *Energy Environ. Sci.* **2014**, *7*, 538.

[7] M. Kammoun, S. Berg, H. Ardebili, *J. Power Sources* **2016**, *332*, 406.

[8] M. F. De Volder, S. H. Tawfick, R. H. Baughman, A. J. Hart, *Science* **2013**, *339*, 535.

[9] L. Nyholm, G. Nyström, A. Mihranyan, M. Strømme, *Adv. Mater.* **2011**, *23*, 3751.

[10] W. Liu, Z. Chen, G. Zhou, Y. Sun, H. R. Lee, C. Liu, H. Yao, Z. Bao, Y. Cui, *Adv. Mater.* **2016**, *28*, 3578.

[11] a) Y. Xu, Y. Zhao, J. Ren, Y. Zhang, H. Peng, *Angew. Chem., Int. Ed.* **2016**, *55*, 7979; b) Y. Zhang, Y. Zhao, J. Ren, W. Weng, H. Peng, *Adv. Mater.* **2016**, *28*, 4524.

[12] a) Y. H. Kwon, S. W. Woo, H. R. Jung, H. K. Yu, K. Kim, B. H. Oh, S. Ahn, S. Y. Lee, S. W. Song, J. Cho, H. C. Shin, J. Y. Kim, *Adv. Mater.* **2012**, *24*, 5192; b) H. Lin, W. Weng, J. Ren, L. Qiu, Z. Zhang, P. Chen, X. Chen, J. Deng, Y. Wang, H. Peng, *Adv. Mater.* **2014**, *26*, 1217.

[13] G. Qian, B. Zhu, X. Liao, H. Zhai, A. Srinivasan, N. J. Fritz, Q. Cheng, M. Ning, B. Qie, Y. Li, S. Yuan, J. Zhu, X. Chen, Y. Yang, *Adv. Mater.* **2018**, *30*, 1704947.

[14] H. Sun, Y. Zhang, J. Zhang, X. Sun, H. Peng, *Nat. Rev. Mater.* **2017**, *2*, 17023.

[15] S. Xu, Y. Zhang, J. Cho, J. Lee, X. Huang, L. Jia, J. A. Fan, Y. Su, J. Su, H. Zhang, H. Cheng, B. Lu, C. Yu, C. Chuang, T. I. Kim, T. Song, K. Shigeta, S. Kang, C. Dagdeviren, I. Petrov, P. V. Braun, Y. Huang, U. Paik, J. A. Rogers, *Nat. Commun.* **2013**, *4*, 1543.

[16] Z. Song, T. Ma, R. Tang, Q. Cheng, X. Wang, D. Krishnaraju, R. Panat, C. K. Chan, H. Yu, H. Jiang, *Nat. Commun.* **2014**, *5*, 3140.

[17] ABAQUS, CAE, "Analysis user's manual, Version 6.12." **2012**.